J Mater Sci (2008) 43:469–474
DOI 10.1007/s10853-007-1829-x

5TH BRAZILIAN MRS MEETING

Production and characterization of sub micrometer hollow Ni–P spheres by chemical reduction: the influence of pH and amphiphilic concentration

C. Bernardi · V. Drago · F. L. Bernardo · D. Girardi · A. N. Klein

Received: 30 January 2007 / Accepted: 8 May 2007 / Published online: 6 September 2007

Abstract Sub micrometer hollow metallic spheres of Ni–P alloy were produced in aqueous solutions at 80 °C by chemical reduction over vesicle templates formed by self-assembling of sodium dodecyl sulfate (SDS) amphiphilic molecules. By varying the pH and SDS concentration (maintaining carefully fixed all other parameters) we obtain different sizes and size distributions, in a monomodal or sometimes bimodal regime. The higher the bath pH the lower the sphere sizes. The sphere shells are nanostructured and the higher the phosphorus content the lower the crystallite sizes. Mass density was of only 3.8 g/cm^3 as a consequence of the hollow morphology and nanostructure. These sphere shells are promising candidates for hydrodesulphurization catalyst due to their high specific area and chemical resistance to sulfur. Characterization was made by XRD, SEM, EDX and thermal analysis.

Introduction

Sub micrometer and nanometer spheres especially those with hollow architecture can exhibit novel properties substantially different from their solid counterparts in the fields of chemistry, physics, biotechnology and materials science, making them attractive for scientific and technological applications. The fabrication of hollow spheres with controlled morphology is especially interesting for applications in catalysts, adsorbents, controlled delivery agents, low density materials and optical, electronic and magnetic devices [1].

The electroless technique is an autocatalytic chemical reduction hydrothermal method for metal deposition without the application of an electrical potential [2]. Recently we used the electroless method to fabricate spherical nanometric particles of Fe–Ni alloys in a large range of stoichiometry [3]. Deng et al. [4] have used this autocatalytic approach for the synthesis of nickel spheres using colloids of $Ni(OH)_2$ as the catalytic sites obtaining spheres with a morphology that can vary from hollow to core-shell to solid.

In this study we are interested in producing hollow metallic Ni–P sub micrometer spheres with the narrowest possible diameter distribution and controlled wall thickness. For this, we used controlled hydrothermal baths where a nickel ion source is initially transformed into a very fine nickel hydroxide gel that adsorbs onto the external surface of a vesicle and is then submitted to an autocatalytic reduction to metallic nickel by the addition of the chemical reducing agent sodium hypophosphite. The vesicle is formed by the self-assembling of the amphiphilic sodium dodecyl sulfate molecules and acts as a template for the nickel deposition. After deposition the vesicle template is removed by vacuum calcination resulting in a hollow sphere of almost pure Ni–P alloy. Because of the rapid kinetics of the deposition and the incorporation of around 20 at.% phosphorus (coming from the hypophosphite decomposition) the formed alloys are nanostructured which differs from the results in Refs. [5, 6]. We also present some results of a crystallization process.

C. Bernardi · A. N. Klein
Departamento de Engenharia Mecânica, Universidade Federal de Santa Catarina, Florianopolis 88040-900, Brazil

V. Drago (✉) · F. L. Bernardo · D. Girardi
Departamento de Física, Universidade Federal de Santa Catarina, Florianopolis 88040-900, Brazil
e-mail: vdrago@fisica.ufsc.br

Experimental

The reagents nickel sulfate $NiSO_4 \cdot 6H_2O$ (Merck), sodium hypophosphite NaH_2PO_2 (Merck), sodium hydroxide NaOH (Riedel) and the anionic amphiphilic sodium dodecyl sulfate (SDS) (Fluka) was used as purchased without further purification.

We prepared two batches of samples both with 0.380 M concentration of the nickel source $NiSO_4 \cdot 6H_2O$ and 0.686 M of sodium hypophosphite. In the first batch the NaOH concentration was fixed at 0.192 M, for three SDS concentrations (0.035, 0.173 and 0.578×10^{-3} M), obtaining the samples named A1, A2 and A3, respectively. In the second batch we used a double NaOH concentration (0.384 M) for the same sequence of SDS concentrations for which the samples are named A4, A5 and A6 as summarized in Table 1.

The methodology for a typical sample preparation, e.g., sample A5, was as follows: 3.000 g of $NiSO_4 \cdot 6H_2O$ and 3 mg of SDS were dissolved in two different beakers each with 15 ml of distilled water. The solution was kept at 80 °C for 5 min under agitation and sonicated for more than 10 min in order to improve the thermal homogenization of the formed vesicles; then an 80 °C solution of 0.920 g of NaOH in 20 ml of distilled water was added drop wise under stirring. The color changes from bright green to milky green due to the formation of a $Ni(OH)_2$ fine gel. Finally, an 80 °C solution of 3.620 g of NaH_2PO_2 in 10 ml distilled water was added under vigorous agitation. After an incubation time (that can vary from 1 min for lower pH to 4 min for the higher pH values) a very rapid expansion (by a factor of ten in volume) with an extremely high hydrogen gas evolution accompanied by the precipitation of fine black particles occurred. At the same time, the color of the solution change from milky green to black. After some seconds, the gas evolution dropped and two minutes later the reaction appeared to have been completed. The final pH of the bath was 4.5 and the precipitate was separated by centrifugation (3000 rpm for 10 min) and then washed sequentially with distilled water, ethanol and acetone. The vesicles templates were then removed by thermal calcination at 100 °C under vacuum for 2 h.

Table 1 Sample identification

Sample name	NaOH concentration (M)	SDS concentration (mM)
A1	0.192	0.035
A2	0.192	0.173
A3	0.192	0.578
A4	0.384	0.035
A5	0.384	0.173
A6	0.384	0.578

For the sample batch A1, A2 and A3 where the NaOH concentration was 0.192 M the final pH of the baths was 3.0; for batch A4, A5 and A6 with 0.384 M NaOH the final pH was between 4.5 and 5.0. The initial pH of the baths cannot be measured due to the immediate formation of the insoluble $Ni(OH)_2$ by addition of NaOH.

Morphological analysis was conducted using a scanning electron microscope, Philips model XL 30, with an EDX facility, model new XL 30, for the chemical analysis. X-ray diffraction (XRD) was carried out on a Philips model X'Pert diffractometer (CuKα radiation $\lambda = 0.154178$ nm, graphite monochomator). Infrared (IR) absorption spectroscopy was performed with a Perkin Elmer model Lambda II spectrometer and the thermal analysis (DSC) with a Shimadzu model DSC–60 differential scanning calorimeter using a heating rate of 10 °C/min in a pure nitrogen atmosphere.

Results and discussion

Figure 1 presents the IR spectra of sample A5 before (Fig. 1a) and after (Fig. 1b) vacuum calcinations. We can observe in Fig. 1a various peaks referring to water and SDS [7] that are absent after calcination, demonstrating the effectiveness of our procedure. TGA analysis (spectra not shown) revealed that the process is accompanied by weight loss that we infer to be due to water and SDS evolution. Similar results were observed for all other samples.

The density of the calcinated spheres measured by gravimetric method was 3.80 g/cm^3 (compare with the 8.90 g/cm^3 for fcc nickel); this low value is a consequence of the structure and hollow morphology of the spheres.

Figure 2 shows the SEM micrographs of the first batch represented by samples A1, A2 and A3. We can observe a well-defined spherical morphology with a smooth surface and low degree of agglomeration for all the samples. The histogram obtained for sample A1 shows a monomodal regime that after being fitted with a normal curve furnished an average diameter of 1.28 ± 0.25 μm; by the EDX chemical analysis the stoichiometry obtained for sample A1 was $Ni_{0.82}P_{0.18}$ (see Table 2). By increasing the SDS amphiphilic concentration by a factor of five, with all other parameters fixed, we obtained sample A2 with a perfect spherical shape, mean diameter of 1.40 μm and a narrow size distribution, characterized by a standard deviation of only 0.14 μm (Table 2). By increasing the SDS concentration further we obtain sample A3 with a bimodal spherical distribution regime reflecting a more complex organization of the surfactant-vesicles formed in our chemical baths.

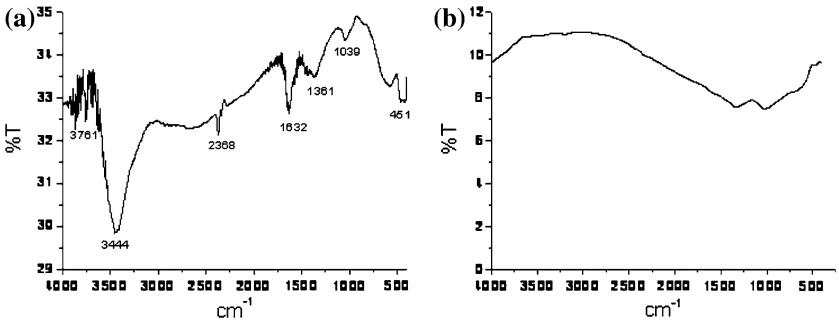

Fig. 1 Infra-red spectra of sample A5 before (**a**) and after (**b**) vacuum calcination

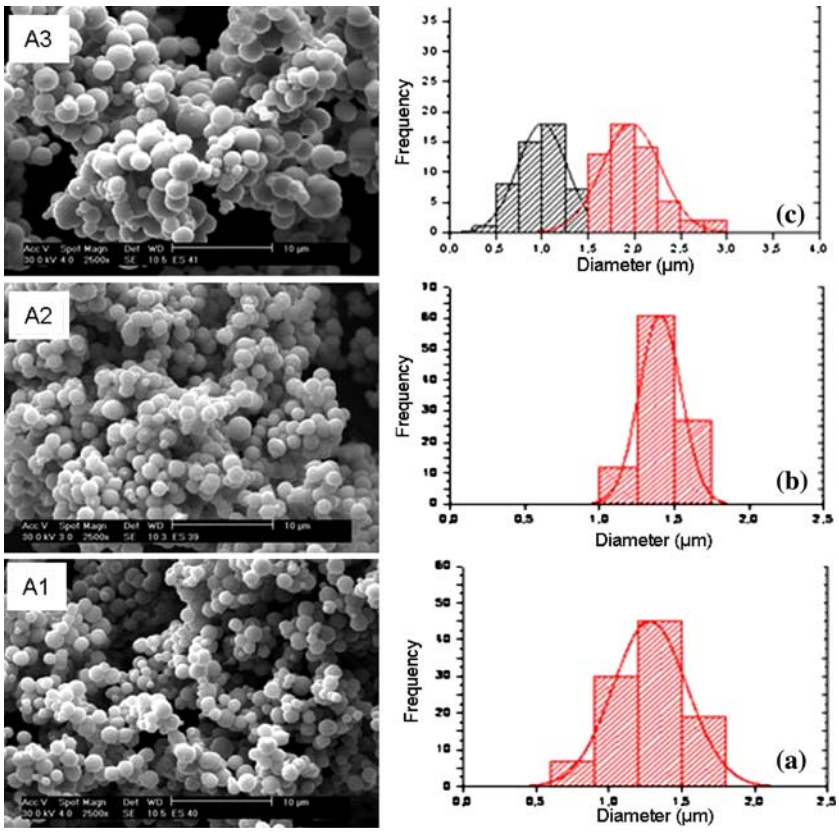

Fig. 2 SEM images of the first batch samples A1, A2 and A3 with NaOH concentration fixed at 0.192 M

In the second batch we doubled the NaOH concentration obtaining the samples named A4, A5 and A6 whose SEM images are shown in Fig. 3. For these cases we also observed a well-defined spherical morphology with a low degree of agglomeration. The regime of diameter distribution appears to be bimodal for A4 (Fig. 3a), monomodal for A5 (Fig. 3b) and bimodal for A6 (Fig. 3c). Average diameters and their standard deviations are given in Table 2. The apparent bimodal regime for sample A4 with the lower SDS concentration is an unexpected result. The average diameter of 0.28 μm obtained for sample A5 (prepared with the higher NaOH and intermediate SDS concentrations) was the shortest obtained for all the six samples. For the intermediate SDS concentration we obtained a monomodal diameter distribution for both pH values with a standard deviation of only 10% in the case of sample A2 (that can be considered as bordering on monodispersive) and of 18% for sample A5. We note a tendency to form smaller vesicles (and consequently

Table 2 Morphology and chemical composition

	Average diameter (μm)	Stoichiometry by EDX	Crystallite size by Scherer (nm)
A1	1.28 ± 0.25	$Ni_{0.82}P_{0.18}$	7.6
A2	1.40 ± 0.14	$Ni_{0.81}P_{0.19}$	5.4
A3	1.00 ± 0.27 and 1.96 ± 0.32	$Ni_{0.82}P_{0.18}$	7.1
A4	0.98 ± 0.38 and 2.50 ± 0.41	$Ni_{0.81}P_{0.19}$	4.8
A5	0.28 ± 0.05	$Ni_{0.77}P_{0.23}$	2.3
A6	0.58 ± 0.16 and 1.91 ± 0.51	$Ni_{0.79}P_{0.21}$	4.4

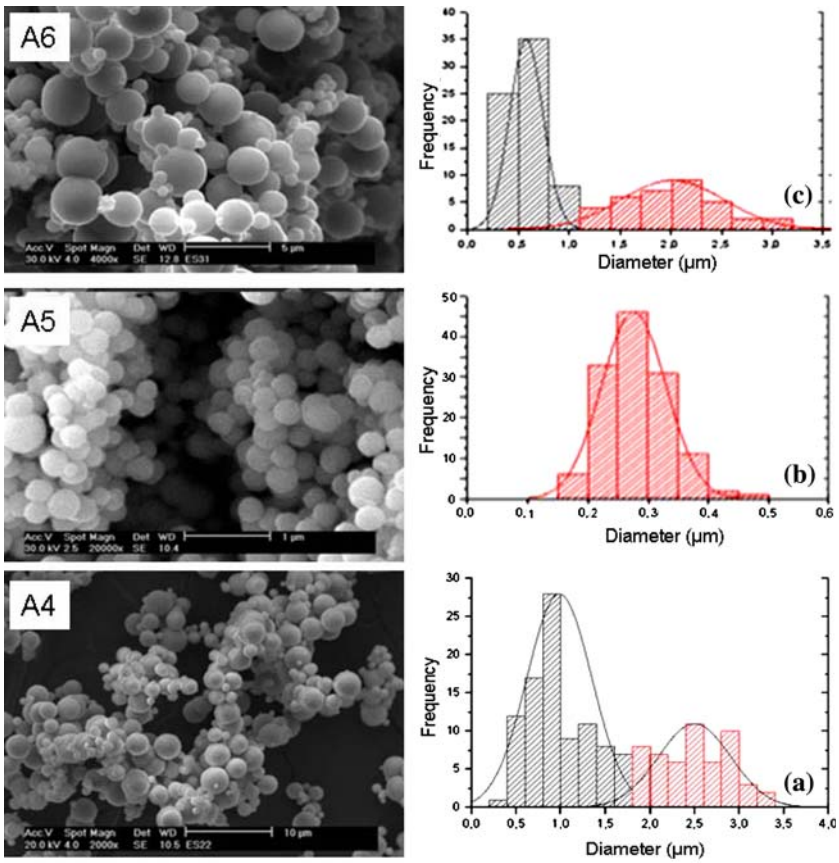

Fig. 3 SEM images of the second batch samples A4, A5 and A6 with the NaOH concentration fixed at 0.384 M

smaller Ni–P spheres) with increasing pH of the baths. Table 2 presents the stoichiometry for all the samples. According to reference [8] the phosphorus content in electroless Ni–P deposits is pH controlled (when the other parameters remain fixed). This was observed for the first sample batch A1, A2, A3 were the% atomic phosphorus range from 18 to 19, which is within our EDX experimental error. However, for the second batch (with 0.384 M NaOH) the at.% P showed a broader range of 19–23 (which we believed to be outside our experimental error) indicating that in this case there is a more complex mechanism of deposition.

The hollow nature of the spheres was evidenced by two methods: by grinding samples in an agate mortar we broke a sphere whose SEM image is in Fig. 4a; and by partial digestion in a 30% HNO_3 solution that corrodes the walls of some spheres as can be seen in the micrograph of Fig. 4b.

The XRD diffraction profiles of the calcinated samples are presented in Fig. 5. In the most of them we can observe evidence for the (111), (200), (220) and (311) reflections of the fcc nickel JCPDS 03-1051 card. The (111) reflection showed a wide angular range of approximately 35°–60° (2Θ) and this is the only reflection present in the sample A5 profile of Fig. 5e. We observed that with increasing phosphorus content the (111) reflection from nickel becomes more broadened, which is an indication of increasing lattice disorder with increasing phosphorus content. The Scherrer formula [9] was used in order to tentatively estimate the crystallite sizes of the samples

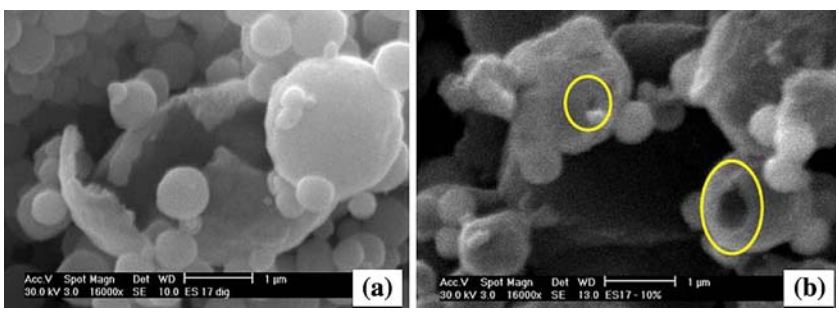

Fig. 4 SEM micrographs showing the hollow nature of the spheres evidenced after grinding (**a**) or a partial digestion in 30% HNO_3 (**b**)

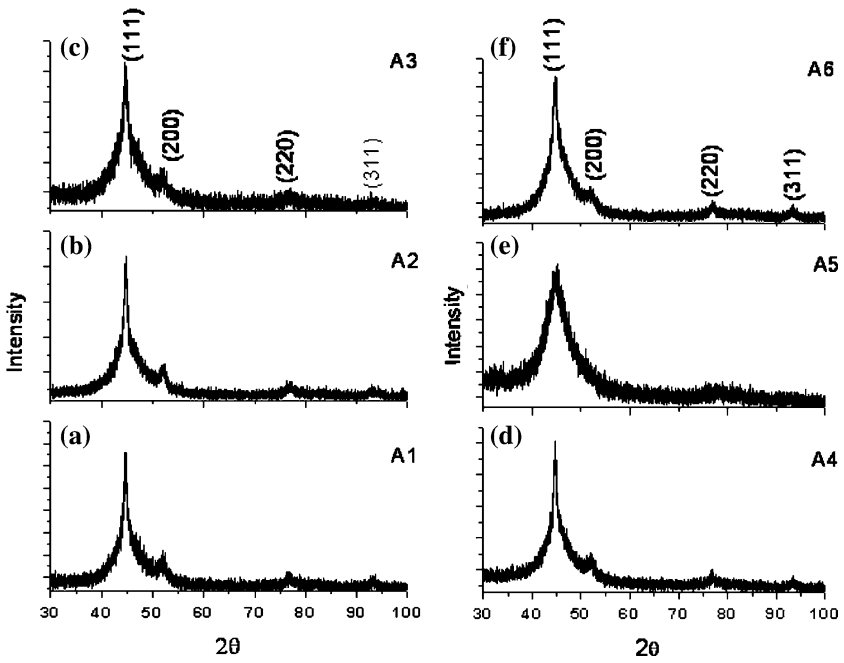

Fig. 5 XRD spectra for the samples A1 (**a**), A2 (**b**), A3 (**c**), A4 (**d**), A5 (**e**) and A6 (**f**); the reflections for planes (111), (200), (220) and (311) of fcc Ni according to the JCPDS 03-1051 card are indicated

(values in Table 2). The higher the phosphorus content the lower the crystallite size. In fact, the (111) reflection can be decomposed into two peaks (analysis not shown); one at $2\Theta = 44.6°$ due to microcrystalline nickel and a second and broader peak as a shoulder at approximately $2\Theta = 47.5°$. The presence of this second reflection has been interpreted as being due to the coexistence of an amorphous phase with a microcrystalline nickel phase [10]. We conclude we have formed nanostructured Ni–P alloys.

The annealing for 3 h at 350 °C in a vacuum gave the typical XRD profile shown in Fig. 6. The amorphous profile disappeared indicating a complete crystallization. We then detected sharp peaks at (2Θ) 44.7°, 51.9°, 76.3°, and 92.8° due to the corresponding (111), (200), (220) and (311) reflections of fcc nickel respectively, plus sharp peaks at (2Θ) 36.3°, 42.7°, 50.6°, 52.7° and 63.4° identified as those belonging to the JCPDS 34-0501 body centered tetragonal Ni_3P precipitate.

The crystallization of the Ni–P hollow spheres was followed by DSC spectra obtained in a flowing nitrogen atmosphere at 10 °C/min (typical curve in Fig. 7). The initial portion of the curve (up to about 300 °C) shows a weak exothermal flux that can be attributed to a relaxation of the amorphous region occurring with minor atomic rearrangements. The sharp and irreversible peak at 350.8 °C is attributed to a crystallization process that according to the XRD results formed a precipitate of two major crystalline phases: fcc nickel and tetragonal Ni_3P.

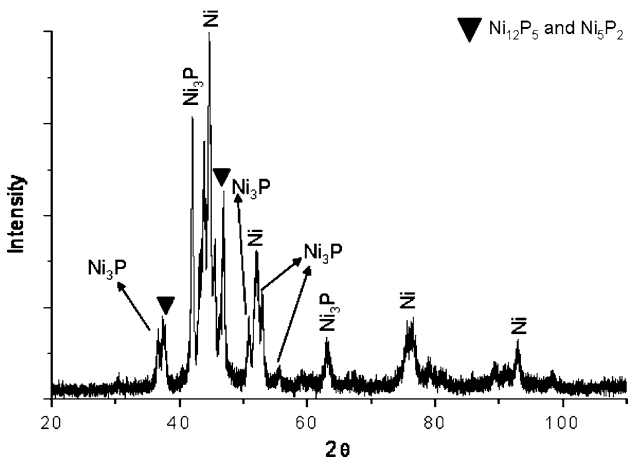

Fig. 6 XRD spectrum for sample A5 after 350 °C/3 h heat treatment

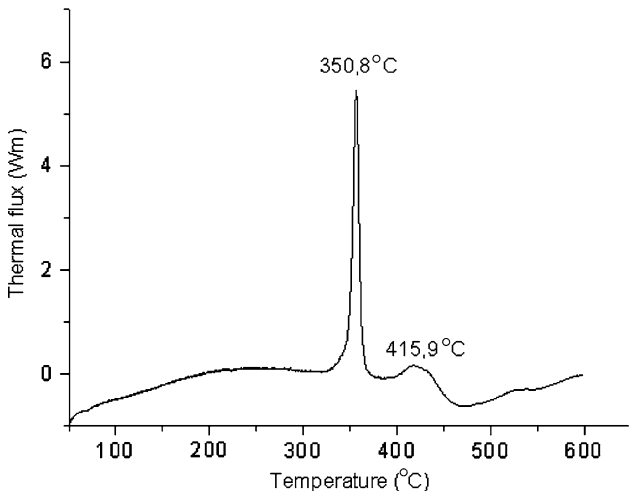

Fig. 7 DSC spectrum for the A5 sample; the exothermal peaks are no longer observed in a second successive run

The second exothermal peak, also an irreversible peak, at 415.9 °C has been attributed in the literature [11] as being due to the formation of the meta stable phases $Ni_{12}P_5$ and Ni_5P_2. Our data are in agreement with this interpretation because the peaks at (2Θ) 37.9° and 47.6° in Fig. 6 can be attributed to these phases. Thus, the thermal behavior is in agreement with the XRD results in the sense that the formed alloys are nanostructured.

Conclusions

Hollow nanostructured sub micrometer nickel-phosphorus spheres were successfully fabricated by autocatalytic reduction over a removable surfactant-vesicle in aqueous solutions at 80 °C. By fixing the concentration of the nickel ion source and that of the chemical reducer we obtain different sizes and regimes of size distribution depending on the NaOH and surfactant concentration. The higher the pH the smaller the spheres. As the concentration of SDS increases we expected an increase in the volume of the vesicles (according to reference [12]) and consequently in the sizes of the nickel spheres with an widening of their size distribution. Ours results do not show exactly this behavior although we controlled carefully all the synthesis parameters. The subject needs further study, in particular to investigate the possibility for two deposition mechanisms; one over the template surfaces and the other by reducing loose $Ni(OH)_2$ agglomerates, particularly in cases where we have a bimodal size distribution. In fact, the complex kinetics of the process can also be inferred from the distinct stoichiometries observed for alloys obtained even at fixed pH.

Acknowledgements We thank the Brazilian agency FINEP and EMBRACO company for its financial support.

References

1. (a) Gubin SP, Yurkov GY, Kataeva NA (2005) Inorg Mat 41:1017; (b) Oyama ST, Wang X, Lee YK, Chun WJ (2004) J Catal 221:263
2. Mallory GO, Hajdu JB (1990) Electroless plating: fundaments and applications. American Electroplaters and Surface Finishers Society, Florida, USA
3. Lima E Jr, Drago V, DeLima JC, Fichtner PFP (2005) J All Comp 396:10
4. Deng Y, Zhao L, Liu L, Shen B, Hu W (2005) Mat Res Bull 40:1864
5. Ni Y, Tao A, Hu G, Cao X, Wei X, Yang Z (2006) Nanotechnology 17:5013
6. Liu Q, Liu H, Han M, Zhu J, Liang Y, Xu Z, Song Y (2005) Adv Mat 17:1995
7. Herzberg G (1945) Infrared and Raman spectra, Van Nostrand Reinhold Company, New York pp 280–282
8. Okinaka Y, Osaka T (1994) In: Gerischer H, Tobias CW (eds) Advances in electrochemical science and engineering, vol 3. VCH
9. Cullity BD (1956) Elements of X-Ray Diffraction, chapter 3. Addison-Wesley
10. Sampath Kumar P, Kesavan Nair P (1996) J Mater Process Technol 56:511
11. Xie S, Qiao M, Zhou W, Luo G, He H, Fan K, Zhao T, Yuan W (2005) J Phys Chem 109:24361
12. Pileni MP (1997) Langmuir 13:3266